ERJ
Engineering Research Journal
Faculty of Engineering
Minoufiya University

FUZZY LOGIC BASED VOLTAGE CONTROL OF A SELF EXCITED INDUCTION GENERATOR DRIVEN BY A VARIABLE SPEED WIND TURBINE

F. E. Abdel Kader and S. A. Deraz

Electrical Engineering Department
Faculty of Engineering-Minoufiya University-Egypt

ABSTRACT

This paper presents a novel fuzzy voltage controller for a stand-alone three-phase self-excited induction generator (SEIG) driven by a variable speed wind turbine. The generated voltage of the SEIG is regulated by adapting the value of excitation capacitance against wind speed and load variations using a fixed capacitor bank and a PWM current controlled voltage source inverter (CC-VSI) with a single capacitor on its DC side. The proposed control scheme consists of two fuzzy logic PI controllers and one hysteresis current controller (HCC). Fuzzy logic based voltage control of the SEIG helps to enhance its performance due to its non-linear adaptive gains, which are varied on-line as the system operating point changes. The need for adaptive regulating scheme comes from the fact that the wind turbine operates over a wide range of operating conditions and therefore the system is highly non-linear. A complete mathematical model of the system is developed in order to study its performance with the proposed controller. Simulation results using Matlab/Simulink software program demonstrate the effectiveness of the proposed controller in regulating the generated voltage of the SEIG against wind speed and load variations.

يقترح هذا البحث أسلوبا للتحكم في جهد المولد التأثيري ذاتي التغذية والمعزول عن الشبكة الكهربية والمدار بواسطة تربينة رياح ذات سرعة متغيرة. يتم ضبط الجهد بضبط قيمة سعة التغذية للمولد ضد تغير سرعة الرياح والحمل عن طريق استخدام وحدة مكثفات ثابتة القيمة مع مغير يتم التحكم فيه بواسطة تعديل عرض النبضة متصل بمكثف ناحية التيار المستمر. تتكون منظومة التحكم من حاكمين غامضين تناسبيين تكامليين وحاكم مقارن للتيار. أسلوب التحكم الغامض يحسن من أداء النظام المقترح وذلك بسبب بارمتراته الغير خطية المتكيفة التي تتغير كلما تغيرت نقطة تشغيل النظام. الحاجة إلى استخدام مثل هذا الأسلوب من التحكم هو أن تربينة الرياح تعمل في مدى واسع من ظروف التشغيل المختلفة ولذلك فان النظام غير خطي بدرجة كبيرة جدا. تم تقديم نموج رياضي كامل للنظام من اجل دراسة أداءه باستخدام الحاكم المقترح. وقد برهنت الدراسة المستفيضة لأداء النظام على فاعلية الحاكم المقترح في ضبط جهد المولد التأثيري ضد تغير سرعة الرياح والحمل.

Keywords: Induction generator, Wind turbine, Fuzzy logic control, Voltage control, Modeling.

1. INTRODUCTION

In recent years, the increasing rate of the depletion of conventional energy sources, degradation of the environmental conditions and the ever increasing need for energy have given rise to an increased emphasis on renewable energy sources such as wind, solar,...etc. A renewable energy source like wind is non-polluting and free in its availability. It is considered as the most cost-competitive of all the environmentally clean and safe renewable energy sources. Use of the induction machine as a generator in wind energy conversion systems, especially in remote and isolated areas, is becoming more and more popular due to its inherent advantages over than known generators [1-3]. However, the main drawback of the induction machine is its need for reactive power to build up the terminal voltage and to generate the electric power. If an appropriate three phase capacitor bank is connected across the machine terminals which is driven by a wind turbine at an appropriate speed and if the rotor of the induction machine has a sufficient residual magnetism, the required reactive power can be generated. This process is called self-excitation [4]. Although the potential of capacitive self-excitation of the induction generator has been recognized for many years, the utility of this method is limited because it has some important drawbacks. One drawback is that the output voltage depends greatly on the induction generator speed and load impedance. Another limitation is that, for a given capacitor value, self-excitation can only be achieved and maintained under certain load and speed combinations. Therefore, the capacitor bank has to be designed according to a defined narrow range of speed and load values. However, even if the capacitor bank is appropriately designed, the machine demagnetizes and stops generating either when the speed falls bellow or the load rises beyond certain values. After that, even with the speed and load returning to their previous

values, the induction generator cannot start working again without the help of an auxiliary energy source and a controller. This means that, although the capacitive self-excitation appears to be the cheapest and simplest technique to be implemented, some additional mechanism has to be added in order to avoid demagnetization and to regulate the generated voltage. Several methods based on different techniques have been presented in order to regulate the generated voltage of the SEIG against load and/or wind speed variations by adapting the value of excitation capacitance. The synchronous condenser is presented in [5] to regulate the voltage of the SEIG against load variations. Although, the high added cost and maintenance requirement of the synchronous condenser over-ride the advantages of the induction generator. The scheme based on switched capacitors [6-7] finds limited application because it regulates the voltage in discrete steps. The schemes based on fixed capacitor thyristor controlled reactor (FC-TCR) and thyristor switched capacitor thyristor controlled reactor (TSC-TCR) [8-9] inject harmonics in the line current of the system which resulting in distorted voltage waveforms and higher losses. To improve the performance of the SEIG, different control strategies using PWM technique have been proposed in [10-14]. However, all of them have some limitations. Some of these proposals use the field oriented control technique, which requires costly and unreliable mechanical position sensing systems such as encoders or resolvers respectively. Moreover, the field oriented control technique depends on the machine parameters which are varied due to operation. The problem of parameters variation is aggravated in generation mode of the induction machine where the magnetizing inductance is naturally varied due to magnetic saturation of the machine. There are other proposals that do not require position-sensing systems. Some of them are based on a shunt-connected PWM voltage source inverter, and some others supplying reactive current to the induction generator by a capacitor bank and an inverter simultaneously based on the instantaneous reactive power theory. However, these proposals have commonly been performed their control action using the conventional PI controllers. Since the system is highly non-linear and the wind turbine operates over a wide range of operating conditions, these schemes do not guarantee an optimal response of the system. This is due to the constant gains of the conventional PI controllers. Moreover, all the previous proposals do not take into account the modeling of the wind turbine. Therefore, the dynamic variation of the turbine output power and the turbine speed (i.e. the generator speed), which have a great effect on the all dynamic characteristics of the system, are not presented. In addition, the d-q model of the SEIG used in these proposals is based on the generalized theory of the induction machine which ignores the effect of iron core loss. This causes large errors in the analysis. Therefore, iron core loss must be taken into account in order to obtain an accurate analysis especially when the induction machine used as a generator.

In this paper a novel fuzzy voltage controller of a stand-alone three-phase SEIG driven by a variable speed wind turbine using a fixed capacitor bank and a PWM current controlled voltage source inverter is presented. A complete mathematical model of the proposed system is developed and simulated in Matlab/Simulink software environment in order to study the performance of the SEIG with the proposed controller.

2. DESCRIBTION OF THE PROPOSED SYSTEM

The main objective of this paper is to propose a new strategy to control the terminal voltage of a stand-alone three-phase SEIG driven by a variable speed wind turbine regarding less the frequency. This is because of uses of the electrical power in such isolated areas include commonly voltage sensitive loads. Such as water heating, space heating and water pumping systems. A schematic diagram of the proposed system is shown in Fig. (1). The proposed system consists of a three-phase induction machine connected to a variable speed wind turbine through a step-up gearbox (1:a). A PWM CC-VSI is connected in parallel with the fixed capacitor bank and load to the AC terminals of the SEIG through a filter reactance. The importance of using the fixed capacitor bank is to eliminate the requirement of pre-charging of the DC side capacitor of the CC-VSI for the start-up process of the induction generator. Also, to reduce the inverter size and thus the controller cost. Moreover, combining the filter inductance and the capacitance of the fixed capacitor bank, a second-order filter is emerged which filters out the high order harmonic components caused by the switching action of the inverter. The CC-VSI is used as a variable source of leading or lagging current in order to control the equivalent excitation capacitance of the SEIG which in turn control the generated voltage of the SEIG against wind speed and load variations. Since the CC-VSI has no real power source on its DC side, a small real power, which is fed from the SEIG, is required to replenish the internal losses of the inverter and to keep the DC side capacitor charged at a specified level in order to make the inverter able to perform its control action properly.

3. PROPOSED CONTROL STRATEGY

The control philosophy used to regulate the terminal voltage of the SEIG is based on the controlled supply

of the output currents of the CC-VSI. As shown in Fig. (1), there are two control loops. The inner control loop forces the actual inverter currents i_i(abc) to follow the reference inverter currents i_i^*(abc) generated by the outer loop through the hysteresis current controller HCC which provides the required switching pluses to the inverter IGBTs switches. The reference inverter currents i_i^*(abc) are derived by adding two orthogonal current components of each phase. The in-phase active current components $i_{\alpha i}^*$(abc) (which represent the real power required to replenish the internal losses of the inverter and to keep the DC side capacitor charged at a specified level) and the quadrature reactive current components $i_{\beta i}^*$(abc) (which represent the reactive power required to regulate the generated voltage). Therefore, the AC voltage of the SEIG is sensed and its magnitude is compared with the reference magnitude (which equals to 220*√2V). The AC voltage error is processed in the first fuzzy logic PI controller (FLC-1). The output of the FLC-1 (i_β^*) of the AC voltage control loop is multiplied by the quadrature unit vectors u_β (abc), which lead the unit vectors of AC voltages by a phase shift of 90°, to give the reference reactive current components $i_{\beta i}^*$(abc) that control the amplitude of the reactive power generated in the CC-VSI. The reference reactive current components lead by a phase shift of 90° the corresponding AC voltages for a positive sign of the AC voltage error. While for a negative sign of the AC voltage error, they lag by a phase shift of 90°. Thus, the CC-VSI operates in capacitive and inductive modes respectively for positive and negative sign of the AC voltage error. Similarly, the in-phase components $i_{\alpha i}^*$(abc) are obtained through the DC voltage control loop. The DC voltage error is processed in the second fuzzy logic PI controller (FLC-2). The output of FLC-2 (i_α^*) is multiplied by the unit vectors u_α (abc) (which in-phase with the corresponding AC voltages of the SEIG) to give the reference active current components $i_{\alpha i}^*$(abc).

4. MODELING OF THE PROPOSED SYSTEM

4.1 Modeling Of The Wind Turbine

The mechanical torque T_t developed by a wind turbine of a blade radius r running in a wind stream of velocity V_w is generally given as [15]:

$$T_t = \frac{1}{2}\,\frac{\rho_a\,\pi\,r^3\,C_p\,V_w^2}{\lambda} \qquad (1)$$

where C_p is known as the power coefficient of the wind turbine, ρ_a is the air density and λ is the tip speed ratio. The C_p is defined as the ratio between the actual power delivered to the free stream power flowing through a similar but uninterrupted area. And λ is the ratio of linear speed at the tip of the blade to the free stream wind speed. It can be given as:

$$\lambda = \omega_t\, r / V_w \qquad (2)$$

where ω_t is the angular turbine speed. A typical relationship between C_p and λ is shown in Fig. (2). It is clear form the figure that, the parameter C_p has a non-linear function with λ. By using a curve-fitting technique, the parameter C_p can be mathematically expressed with a polynomial function of seventh degree as a function of λ which given as follows:

$$C_p = a_7\lambda^7 + a_6\lambda^6 + a_5\lambda^5 + \ldots + a_2\lambda^2 + a_1\lambda + a_0 \qquad (3)$$

where a_7, a_6,...., a_0 are constants and are given in the Appendix.

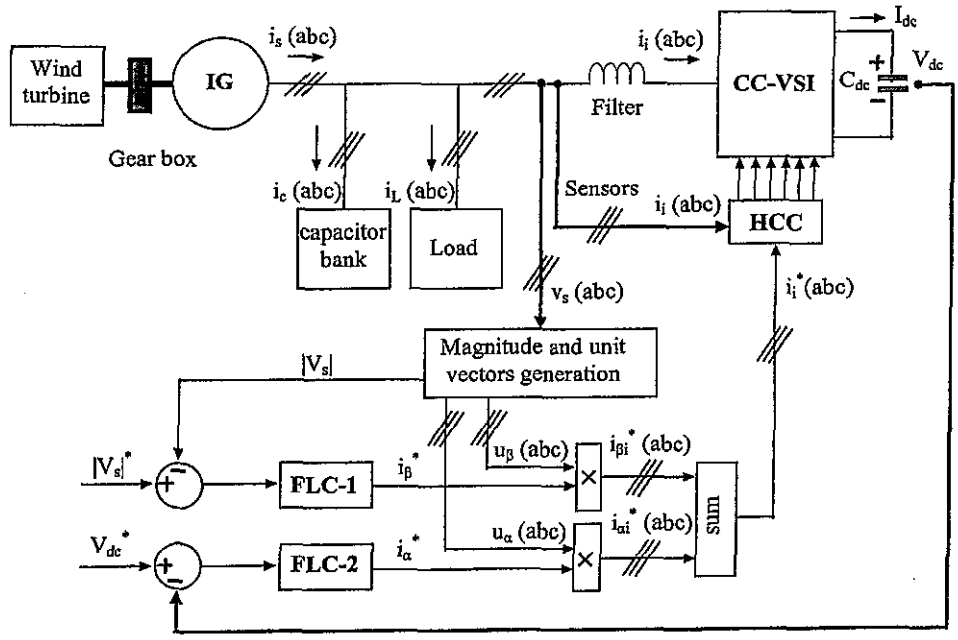

Fig. (1) A schematic diagram of the proposed system

4.2 Modeling Of The SEIG

The d-q model of the SEIG is helpful to analyze its all characteristics. To model the SEIG effectively, the parameters of the induction machine should be measured accurately. The traditional tests (no-load and short circuit) are used to get these parameters. For motoring application, these parameters can be used directly. However, for SEIG application the variation of the magnetizing inductance should be taken into account. Because it is the main factor in voltage buildup and stabilization of the generated voltage. The relation between the magnetizing inductance and the magnetizing current is obtained experimentally and depicted in Fig. (3). This relation can be mathematically represented by a sixth order curve fit as follows:

$$L_m = b_6 i_m^6 + b_5 i_m^5 + ... + b_1 i_m + b_0 \quad (4)$$

where $b_6, b_5, ..., b_0$ are constants which given in the Appendix. Since, the magnetization characteristics of the SEIG are non-linear due to saturation and the magnetizing inductance depends on the instantaneous value of the magnetizing current. Thus, the magnetizing current must be calculated at each step of the simulation in order to evaluate the corresponding instantaneous value of the magnetizing inductance.

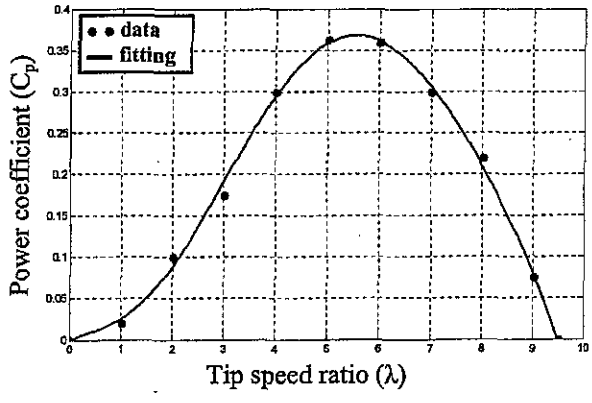

Fig. (2) Power coefficient curve

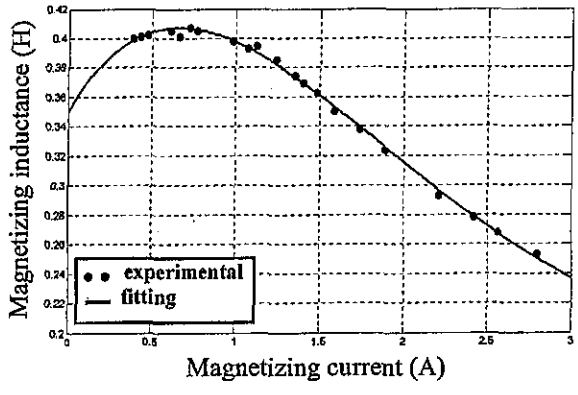

Fig. (3) Experimental variation of the magnetizing inductance with the magnetizing current

Magnitude of the magnetizing current can be calculated as follows:

$$i_m = \sqrt{i_{dm}^2 + i_{qm}^2} \quad (5)$$

Fig. (4) shows the equivalent circuit of the SEIG with the proposed controller in the d-q stationary reference frame. The effect of iron core loss is taken into account in order to obtain an accurate model and in turn an accurate analysis. The effect of iron core loss is expressed by a resistance (R_m) connected in parallel with the magnetizing branch. The reference directions of the currents in the d-q model, which are based on the generalized machine theory, are changed into the directions shown in Fig. (4) in order to be more convenient in studying the generator characteristics. The mathematical equations that describe the SEIG model in the d-q stationary reference frame are derived and can be given as follows:

$$v_{ds} = -R_s i_{ds} + \rho\varphi_{ds} \quad (6)$$

$$v_{qs} = -R_s i_{qs} + \rho\varphi_{qs} \quad (7)$$

$$0 = R_r i_{dr} + \omega_r \varphi_{qr} + \rho\varphi_{dr} \quad (8)$$

$$0 = R_r i_{qr} - \omega_r \varphi_{dr} + \rho\varphi_{qr} \quad (9)$$

$$R_m i_{dfe} = \rho\varphi_{dm} \quad (10)$$

$$R_m i_{qfe} = \rho\varphi_{qm} \quad (11)$$

$$i_{dr} = i_{ds} + i_{dm} + i_{dfe} \quad (12)$$

$$i_{qr} = i_{qs} + i_{qm} + i_{qfe} \quad (13)$$

$$\varphi_{ds} = -L_{ls} i_{ds} + L_m i_{dm} \quad (14)$$

$$\varphi_{qs} = -L_{ls} i_{qs} + L_m i_{qm} \quad (15)$$

$$\varphi_{dr} = L_{lr} i_{dr} + L_m i_{dm} \quad (16)$$

$$\varphi_{qr} = L_{lr} i_{qr} + L_m i_{qm} \quad (17)$$

$$\varphi_{dm} = L_m i_{dm} \quad (18)$$

$$\varphi_{qm} = L_m i_{qm} \quad (19)$$

$$T_e = \frac{3p}{4}(\varphi_{ds}(i_{qs} + i_{qfe}) - \varphi_{qs}(i_{ds} + i_{dfe})) \quad (20)$$

The equation of motion is given as:

$$\frac{T_t}{a} = T_e + j\frac{d\omega_m}{dt} = T_e + j\left(\frac{2}{p}\right)\frac{d\omega_r}{dt} \quad (21)$$

where subscripts d and q are used to indicate direct and quadrature axis respectively. Subscripts s, r, m and fe are used to indicate stator, rotor, magnetizing and iron core loss variables respectively. Variables v, i and φ represents the instantaneous voltage, current and flux respectively. R_s and R_r are the stator and rotor resistance respectively. L_{ls} and L_{lr} are the leakage stator and rotor inductance respectively. ω_r and ω_m are electrical and mechanical angular generator speed respectively. ρ is the time derivative. p is the number of poles and T_e is the electromagnetic torque of the SEIG. j is the effective inertia of the

system. The SEIG and the wind turbine parameters are given in the Appendix.

4.3 Modeling Of The Load And Fixed Capacitor Bank

The voltage-current equations of the fixed excitation capacitor bank in the d-q stationary reference frame can be written as follows:

$$\rho v_{ds} = \frac{i_{dc}}{C} \quad (22)$$

$$\rho v_{qs} = \frac{i_{qc}}{C} \quad (23)$$

where C is the per phase capacitance of the fixed capacitor bank. i_{dc} and i_{qc} are the direct and quadrature axis components of the fixed capacitor bank current respectively. These components can be calculated as follows:

$$i_{dc} = i_{ds} - i_{dL} - i_{di} \quad (24)$$

$$i_{qc} = i_{qs} - i_{qL} - i_{qi} \quad (25)$$

where i_{di} and i_{qi} are the direct and quadrature axis components of the AC side inverter current respectively. While i_{dL} and i_{qL} are the direct and quadrature axis components of the load current respectively.

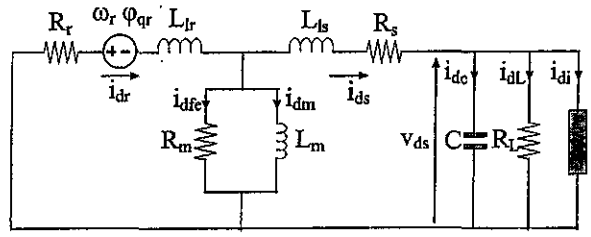

(a) d-axis

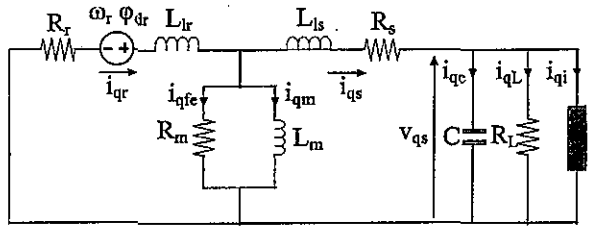

(b) q-axis

Fig. (4) Equivalent circuit of the proposed system

4.4 Modeling Of The CC-VSI

The voltage equation that describes charging and discharging of the DC side capacitor of the CC-VSI can be written as follows:

$$\rho V_{dc} = I_{dc} / C_{dc} \quad (26)$$

Where V_{dc} is the voltage across the DC side capacitor C_{dc} of the CC-VSI and I_{dc} is the current passing through it as shown in Fig. (5). The reference value of the DC voltage V_{dc}^* is chosen such that, it must be greater than the peak value of the generated AC line voltage of the SEIG in order to obtain adequate control of the CC-VSI currents. The DC current I_{dc} can be expressed in terms of switching functions of the inverter as follows [10]:

$$I_{dc} = SA\ i_{ai} + SB\ i_{bi} + SC\ i_{ci} \quad (27)$$

where SA, SB, SC are switching functions stating the ON/OFF positions of the inverter IGBTs switches. The switching function SA takes the value of 1 when the upper switch is ON and the lower switch is OFF in the inverter leg of phase A. Its value is 0 when the upper switch is OFF and the lower switch is ON. Similar logic is applied for the other two phases (phase B and phase C). Instantaneous phase voltages e_a, e_b, e_c generated by the inverter can also be expressed in terms of switching functions as [12]:

$$e_a = (V_{dc}/3)(2SA - SB - SC) \quad (28)$$

$$e_b = (V_{dc}/3)(2SB - SA - SC) \quad (29)$$

$$e_c = (V_{dc}/3)(2SC - SA - SB) \quad (30)$$

As shown in Fig. (5), the three phase AC inverter currents i_{ai}, i_{bi}, i_{ci} can be determined as follows:

$$\rho i_{ai} = (v_a - e_a - i_{ai} R_f)/L_f \quad (31)$$

$$\rho i_{bi} = (v_b - e_b - i_{bi} R_f)/L_f \quad (32)$$

$$\rho i_{ci} = (v_c - e_c - i_{ci} R_f)/L_f \quad (33)$$

where v_a, v_b, v_c are the instantaneous three phase stator voltages of the SEIG. R_f and L_f are the per phase filter resistance and inductance respectively.

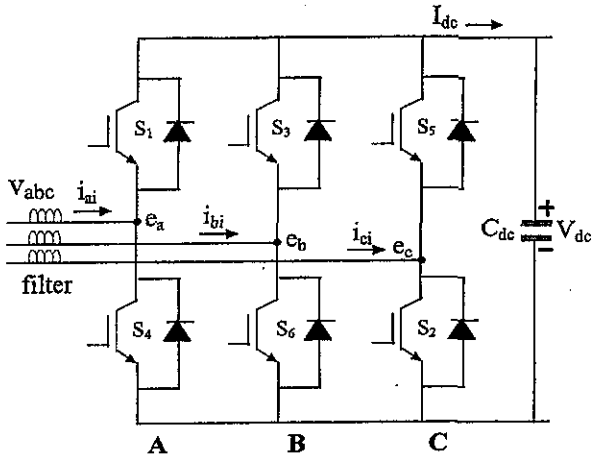

Fig. (5) A schematic diagram of the CC-VSI

4.5 Modeling Of The HCC

The switching functions (SA, SB and SC) stating the on/off positions of the inverter IGBTs switches which are generated form the hysteresis current comparator can be mathematically expressed as follows [12]:

If $i_{ai} < (i_{ai}^* - hb)$ switch s_1 off and switch s_4 on. SA=0
If $i_{ai} > (i_{ai}^* + hb)$ switch s_1 on and switch s_4 off. SA=1
If $i_{bi} < (i_{bi}^* - hb)$ switch s_3 off and switch s_6 on. SB=0
If $i_{bi} > (i_{bi}^* + hb)$ switch s_3 on and switch s_6 off. SB=1
If $i_{ci} < (i_{ci}^* - hb)$ switch s_5 off and switch s_2 on. SC=0
If $i_{ci} > (i_{ci}^* + hb)$ switch s_5 on and switch s_2 off. SC=1

where hb is the current band of hysteresis current controller HCC.

5. FUZZY LOGIC CONTROL

Fuzzy logic based voltage control of the system helps to enhance the system performance over than conventional PI controller. This is due to its non-linear adaptive gains, which are varied on-line as system operating point changes. The need for adaptive regulating scheme comes from the fact that the wind turbine operates over a wide range of operating conditions and therefore the system is highly non linear. The proposed system has two fuzzy logic PI controllers. The FLC-1 is used in the AC voltage control loop while the other FLC-2 is used in the DC voltage control loop. Fig. (6) shows the block diagram of the FLC-1, where it consists of three main blocks: fuzzification, evaluation of control rules and defuzzification. The AC voltage error E and change in this error CE are the crisp inputs of the FLC-1. The input signals E and CE are converted to the corresponding per unit signals e and ce (through dividing by the input scaling factors GE and GC respectively). The input signals e and ce are expressed in fuzzy set notation using linguistic labels

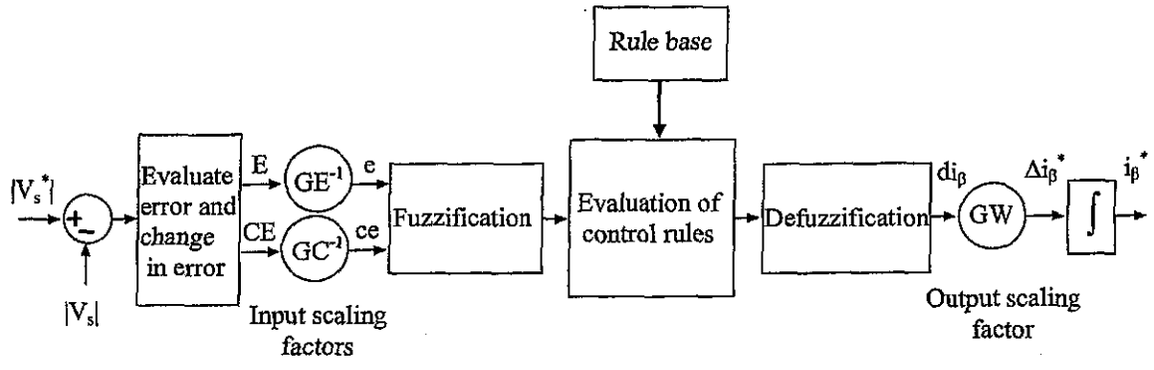

Fig. (6) Block diagram of FLC-1

characterized by membership grades before being processed by the fuzzy logic controller. Also, the output signal di_β is expressed in fuzzy set notation using linguistic labels characterized by membership grades. The membership functions MFs for e, ce and di_β are shown in Fig. (7). There are seven MFs for both e and ce signals, whereas there are nine MFs for the output di_β. Table (1) shows the corresponding rule base of the FLC-1. The top row and left column of the table indicate the fuzzy sets of the variables e and ce respectively. While, the MFs of the output variable di_β are shown in the body of the table. There are 49 possible rules, which are used to decide the appropriate control action. In the implementation of the fuzzy logic controller, the input variables e and ce are fuzzified, the control rules are evaluated and finally the fuzzy output is defuzzified. The crisp output of the FLC-1 di_β is converted to Δi_β^* by multiplying by the output scaling factor GW. This signal is accumulated to generate the actual command value i_β^*. Using a similar technique, the FLC-2 is implemented. The fuzzy logic PI controller can be considered as a conventional PI controller but with non linear adaptive gains. Therefore, its advantage is obvious, since the values of Δi_α^* and Δi_β^* which are used to decide the appropriate control action are adaptive for the DC and AC voltage errors respectively. Therefore, an optimal dynamic response of the proposed system is achieved.

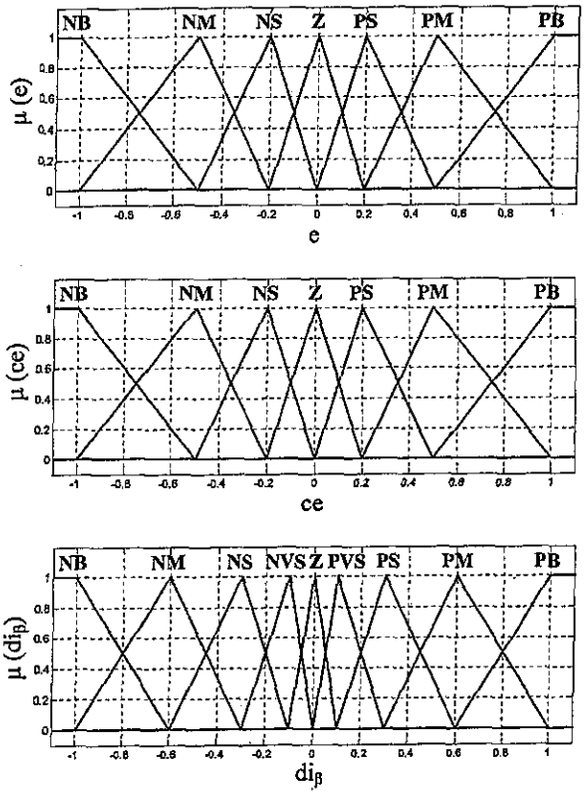

Fig. (7) Membership functions of the FLC-1

Table (1) Rule base of the FLC-1

ce \ c	NB	NM	NS	Z	PS	PM	PB
NB	NB	NB	NB	NM	NS	NVS	Z
NM	NB	NB	NM	NS	NVS	Z	PVS
NS	NB	NM	NS	NVS	Z	PVS	PS
Z	NM	NS	NVS	Z	PVS	PS	PM
PS	NS	NVS	Z	PVS	PS	PM	PB
PM	NVS	Z	PVS	PS	PM	PB	PB
PB	Z	PVS	PS	PM	PB	PB	PB

6. RESULTS AND DISCUSSION

The proposed system is modeled and simulated using Matlab/Simulink software program in order to study its performance with the proposed controller. Fig. (8) shows the simulink model of the proposed system, which consists of different blocks called subsystems. Each subsystem performs a specific task. In the first, the induction machine is driven by the wind turbine from the rest with a wind velocity of 6.5 m/sec. After the speed of the induction machine reaches to its steady state value, the fixed capacitor bank and the CC-VSI are connected across the machine terminals at t=0 sec in order to excite the induction machine under no-load condition.

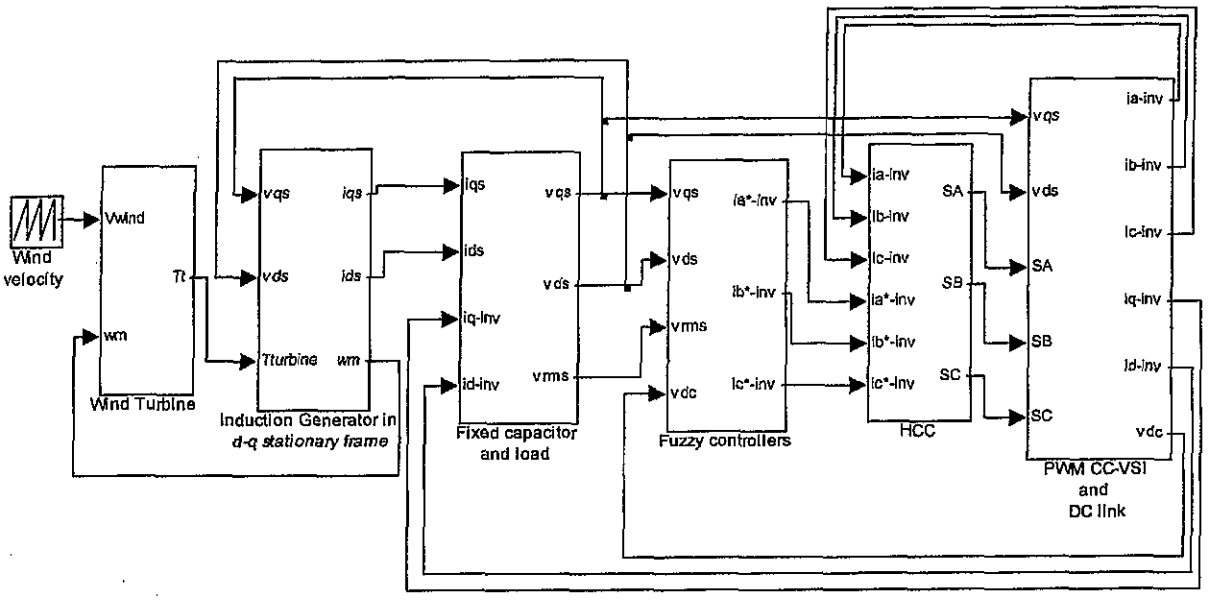

Fig. (8) Simulink model of the proposed system

The fixed capacitor bank is selected with a value of 10 μF in order to sustain the generated voltage of the SEIG under no-load condition and to reduce the inverter size. Fig. (9) shows the dynamic response of the system during the start up process and switching in the controller under no-load condition. Firstly, the terminal voltage of the SEIG settles to 275.05V(RMS), whereas the DC side capacitor of the CC-VSI is also charged (due to the anti-parallel diodes across the inverter IGBTs) to 643.14V as shown in Fig. (9.a) and Fig. (9.b) respectively. However, the DC voltage does not reach its reference value whish is set to 750V and the terminal voltage is over-excited whose reference voltage is set to 220V(RMS). When the controller is brought into operation by giving it a switching pulse at t=3 sec, the over-excited terminal voltage and the DC side voltage are regulated to their reference values by controller action. In this case, the CC-VSI is operated in inductive-mode where the reactive component of the inverter current lags the voltage of the SEIG by a phase shift of 90° as shown in Fig. (9.c). Fig. (9.d) shows the dynamic response of the stator current which is decreased after the controller starts its operation. This is due to that, operation of the inverter in inductive mode reduces the equivalent excitation capacitance of the SEIG which in turn reducing the stator current. Also for this reason, the generator losses are reduced and therefore the extracted power form the wind turbine which equals the generator input power is reduced as shown in Fig. (9.e). This increases the generator speed after switching in the controller as shown in Fig. (9.f). Fig. (9.g) shows the zoomed dynamic response of the actual and reference inverter currents of phase (A). It is clear from the figure that, the HCC forces the actual inverter current to follow its reference in a hysteresis current band.

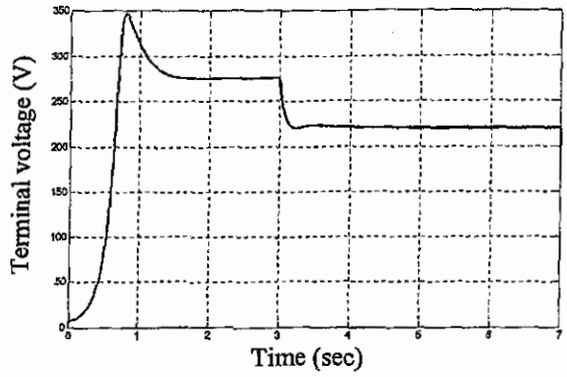

(a) Terminal voltage response

(b) DC side voltage response

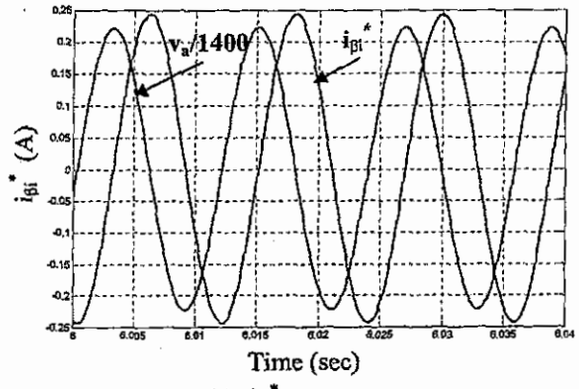

(c) $i_{\beta i}^*$ response

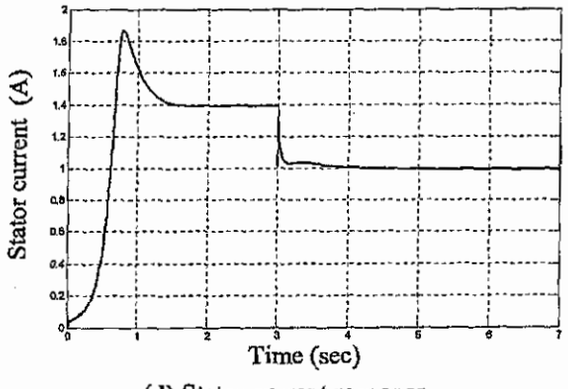

(d) Stator current response

Fig. (9) (continued)

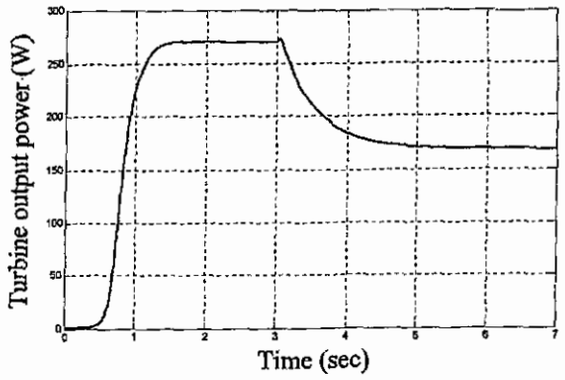

(e) Turbine output power response

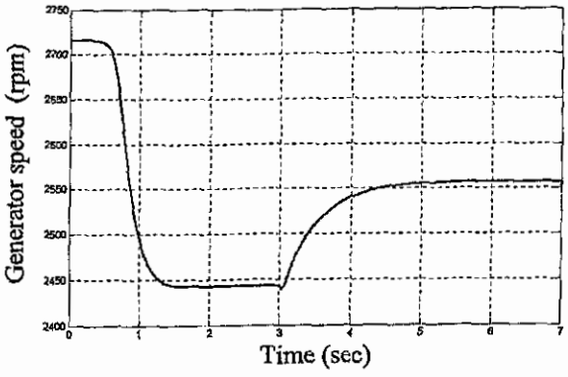

(f) Generator speed response

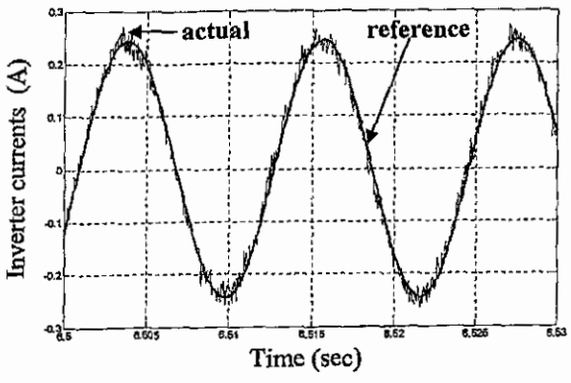

(g) Actual and reference inverter currents response

Fig. (9) System response during start-up and switching in the controller

Fig. (10) shows the dynamic response of the system under sudden loading with load resistance (R_L= 450Ω) at t=7 sec. In this case, the CC-VSI which is in the inductive mode in the previous case (no-load condition), changes to operate in the capacitive mode in order to inject the required reactive power to regulate the generated voltage as shown in Fig. (10.c). After that, the system is subjected to a sudden increase in load resistance from the previous value to (R_L= 650Ω) at t= 15 sec.

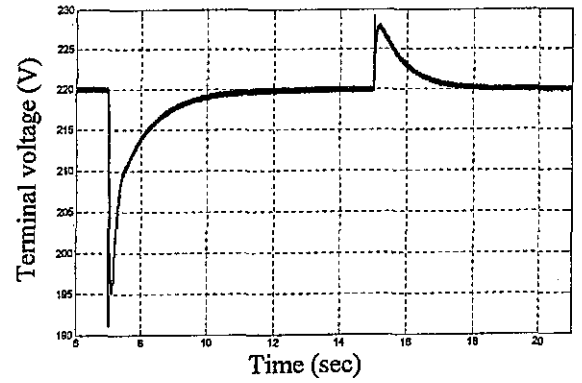

(a) Terminal voltage response

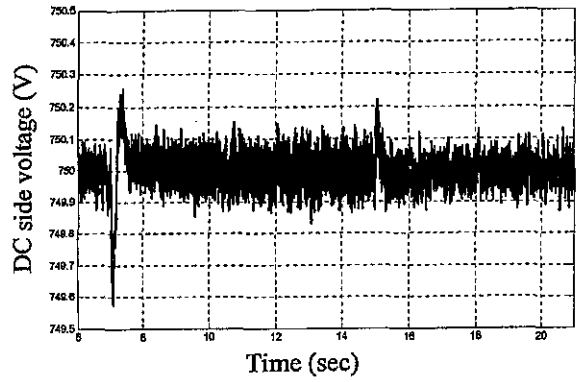

(b) DC side voltage response

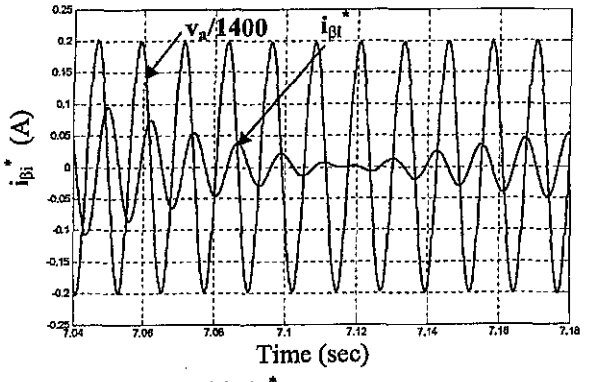

(c) $i_{\beta i}^*$ response

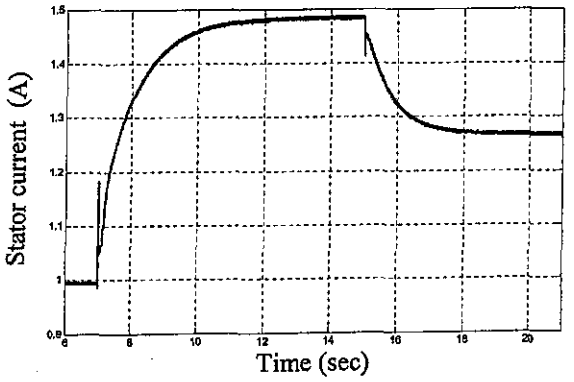

(d) Stator current response

Fig. (10) (continued)

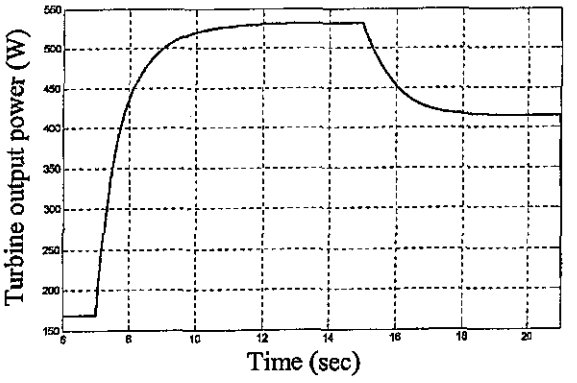

(e) Turbine output power response

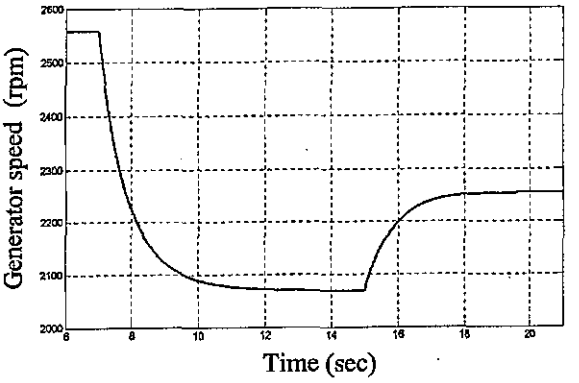

(f) Generator speed response

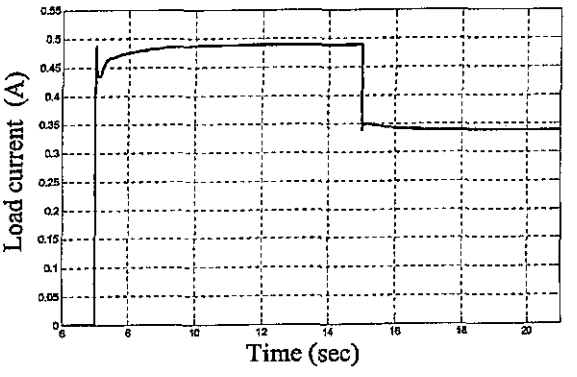

(g) Load current response

Fig. (10) System response during sudden decrease and increase in the load resistance

Fig. (11) shows the dynamic response of the system for sudden decrease in the wind speed from 6.5 m/sec to 6 m/sec at t=21 sec. Followed by a sudden increase from 6 m/sec to 7 m/sec at t=30 sec. The obtained results, which are shown in Fig. (10) and Fig. (11), demonstrate the effectiveness of the proposed controller for regulating the generated voltage of the SEIG under wind speed and load variations.

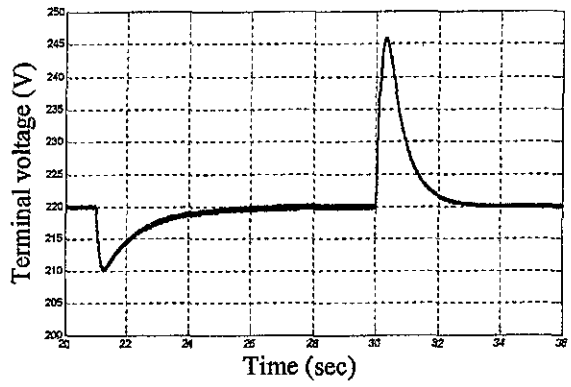

(a) Terminal voltage response

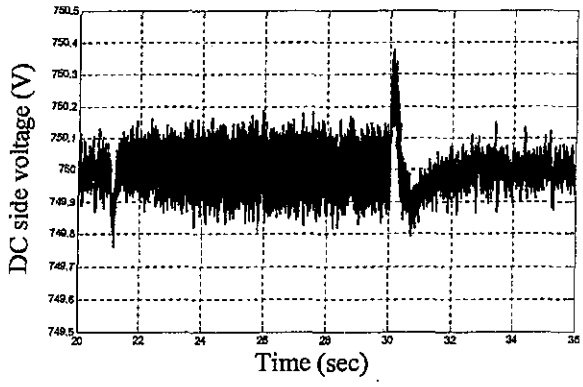

(b) DC side voltage response

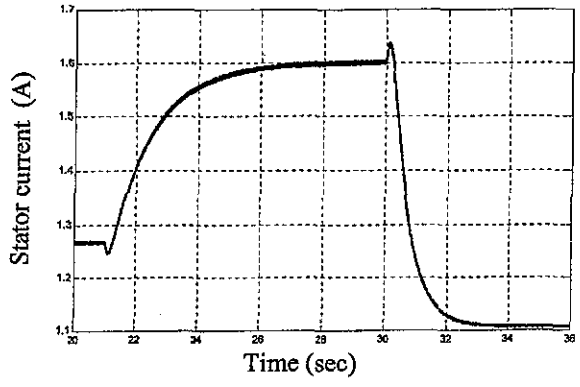

(c) Stator current response

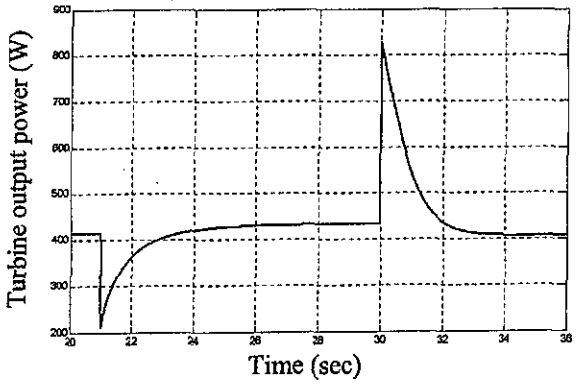

(d) Turbine output power response

Fig. (11) (continued)

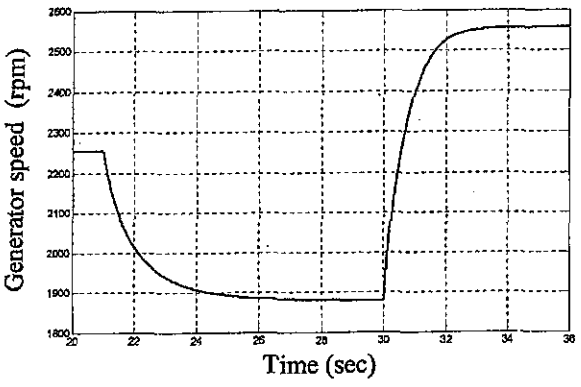

(e) Generator speed response

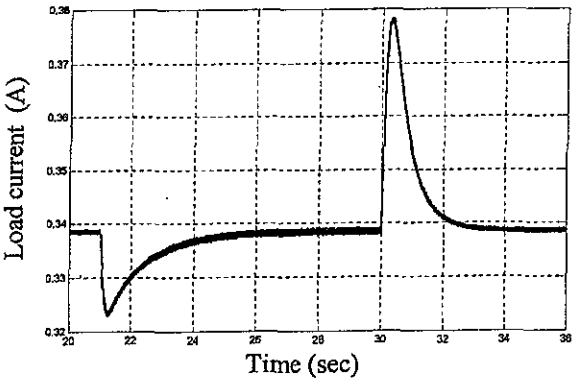

(f) Load current response

Fig. (11) System response during sudden decrease and increase in wind velocity

Fig. (12) shows the steady state operating points of the system for the previous operating conditions on the turbine output power/speed characteristics. The steady state operating points are characterized by the moment of settlement.

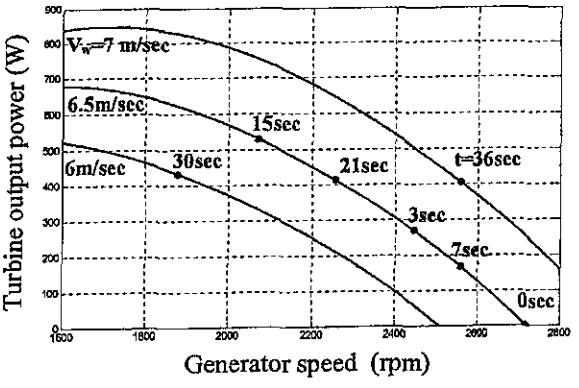

Fig. (12) Steady state operating points of the system on the turbine output characteristics

7. CONCLUSION

A novel fuzzy logic controller in order to regulate the generated voltage of a stand-alone SEIG driven by a variable speed wind turbine is presented. The main innovations presented in this work are the modeling of the system and the control strategy. The fixed capacitor bank and the CC-VSI are used to accomplish the required reactive power in order to regulate the generated voltage of the SEIG under wind speed and load variations. The inclusion of the fixed capacitor bank eliminates the requirement of pre-charging of the DC side capacitor of the CC-VSI for the start-up process of the induction generator and supports minimizing the inverter current. This reduces the inverter rating. Moreover, The implementation of the proposed controller neither requires the use of a mechanical position nor a speed-sensing system. This increases the system reliability. These two features enable reduced costs of the proposed control scheme. Moreover, the proposed controller is insensitive to parameters variation and is adaptive to changes in the operating conditions. Therefore, it has an optimal dynamic response. Simulation results using Matlab/Simulink demonstrate the effectiveness of the proposed controller in regulating the terminal voltage of the SEIG against wind speed and load variations.

8. APPENDIX

-The induction machine used in this study is a 3-phase, 4 poles, 1.1 Kw. The machine parameters are R_s=6.396 Ω, R_r=7.965 Ω, L_{ls}= L_{lr}=20.837 mH, R_m=933.61 Ω, j_m=0.015 kg.m^2.
-The wind turbine parameters are: r=1.85 m, gear ratio= 1:8.53, j_t=1.6384 kg.m^2
-The equivalent system inertia j=0.03452 kg.m^2.
-Constants of Equation (3) are: a_7= 4.6324e-7, a_6= -3.5767e-5, a_5= 8.0176e-4, a_4= -7.5748e-3, a_3= 0.0289, a_2= -0.025952, a_1= 0.029343, a_0= -7.255e-4.
-Constants of Equation (4) are: b_6= -3.8493e-5, b_5= 0.00109534, b_4= -0.0126716, b_3= 0.0741395, b_2= -0.213417, b_1= 0.198004, b_0= 0.350224
-The hysteresis band current controller hb=0.01.
-Filter parameters are: R_f=0.1 Ω, L_f=0.055 H.

9. REFERENCES

[1] D. F. Warne, P. G. Calnan, "Generation of electricity from the wind", IEE Proceedings, Vol. 124, No. 11R, pp. 963-985, Nov. 1977.

[2] R. Chaturvedi, S. S. Murthy, "Use of conventional induction motor as a wind driven self excited induction generator for autonomous operation", IEEE Transactions on energy conversion, pp. 2051-2055, Apr. 1989.

[3] S. S. Murthy, B. P. Singh, C. Nagamani, K. V. V. Satyanarayana, "Studies on the use of conventional induction motor as self excited induction generators", IEEE Transactions on energy conversion, Vol. 3, No. 4, pp. 842-848, Dec. 1988.

[4] J. M. Elder, J. L. Woodward, "The process of self excitation in induction generators", IEE proc., Vol. 130, Pt. B, No. 2, pp. 103-107, Mar. 1983.

[5] B. T. Ooi, R. A. David, "Induction-generator / synchronous-condenser system for wind turbine power", IEE Proceedings, Vol. 126, No. 1, pp. 69-74, Jan. 1979.

[6] S. P. Singh, B. Singh, M. P. Jain, "Performance characteristics and optimum utilization of a cage machine as capacitor excited induction generator", IEEE Transactions on energy conversion, Vol. 5, No. 4, pp. 679-684, Dec. 1990.

[7] S. A. Daly, A. M. de Paor, R. J. Simpson, "Modelling and control of a wind driven induction generator for water storage heating", IEE Proceedings, Vol. 130, Pt. A, No. 9, pp. 596-601, Dec. 1983.

[8] T. Ahmed, O. Noro, E. Hiraki, M. Nakaoka, "Terminal voltage regulation characteristics by static VAR compensator for a three-phase self-excited induction generator", IEEE Transactions on Industry Applications, Vol. 40, No. 4, pp. 978-988, July/Aug. 2004.

[9] M. B. Brennen, A. Abbondanti, "Static exciter for induction generators", IEEE Transactions on industry applications, Vol. IA-13, No. 5, pp. 422-428, Sep./Oct. 1977.

[10] S. C. Kuo, L. Wang, "Analysis of voltage control for a self excited induction generator using a current controlled voltage source inverter (CC-VSI)", IEE Proceedings, Vol. 148, No. 5, Sep. 2001.

[11] D. Seyoum, M. F. Rahman, C. Grantham, "Inverter supplied voltage control system for an isolated induction generator driven by a wind turbine", IEEE Industry applications conf., Vol. 1, pp. 568-575, Oct. 2003.

[12] A. kishore, R. C. Prasad, B. M. Karan, "Design of field oriented controller to improve dynamic characteristics of three phase self excited induction generator", Proceedings of the IEEE-ICIEA conf., pp. 312-318, 2006.

[13] S. R. Silva, R. O. C. Lyra, "PWM converter for excitation of induction generators", The European power electronics association, pp. 174-178, 1993.

[14] S. Wekhande, V. Agarwal, "Simple control for a wind-driven induction generator", IEEE Transactions on Industry Applications, Vol. 7, Issue 2, pp. 44-53, Mar/Apr 2001.

[15] M. R. Patel, "Wind and solar power systems", [book], CRC press, 1999.